5639966

QUASISTATIC VS. DYNAMIC MODULUS MEASUREMENTS OF PLASMA-SPRAYED THERMAL BARRIER COATINGS

J.I. Eldridge, G.N. Morscher, and S.R. Choi
NASA Glenn Research Center
Cleveland, OH 44135

ABSTRACT

Plasma-sprayed 8wt% yttria-stabilized zirconia (8YSZ) thermal barrier coatings (TBCs) have been demonstrated to exhibit nonlinear hysteretic elastic behavior by quasistatic cyclic compression and cylindrical punch indentation measurements. In particular, the instantaneous (tangential) elastic modulus increases with applied stress and exhibits significant hysteresis during cycling. Sound velocity (dynamic) measurements also show an increase in TBC modulus with applied compressive stress, but in contrast, show no significant hysteresis for the modulus during cycling. The nonlinear elastic behavior of the TBCs evidenced by these tests is attributed to coating compaction and internal sliding. The differences between the quasistatic and dynamic measurements are explained by the relative absence of the effect of internal sliding in the dynamic modulus measurements. By incorporating short load reversals into the larger loading cycle and measuring the instantaneous modulus at the start of each load reversal, the effects of internal sliding can be substantially reduced in the quasistatic measurements, and the resulting modulus values show good agreement with the modulus values determined by dynamic sound velocity measurements.

INTRODUCTION

High compliance is desirable to enable thermal barrier coatings (TBCs) to achieve their required high strain tolerance, therefore reliable methods are needed to measure their elastic response. Complications in determining an elastic modulus arise due to the defect-rich (voids and cracks) microstructure of plasma-sprayed coatings (Fig. 1); the effective modulus is dominated by the elastic response of these defects, leading to highly nonlinear and hysteretic elastic behavior.[1-4] This behavior has resulted in a wide range of elastic modulus values reported for TBCs as determined by different methods. Apparent inconsistencies are not surprising since the effective elastic modulus will depend on the applied stress and stress history. In particular, a distinction can be made between quasistatic and dynamic modulus measurements. Quasistatic modulus measurements are determined during slowly varying, high strain amplitude, monotonic loading or unloading. Examples presented here are uniaxial compression testing and indentation. In contrast, dynamic modulus measurements are determined during low strain amplitude, high frequency, oscillatory stress/strain cycling such as occurs during sound wave propagation. While the quasistatic and dynamic modulus measurements show good agreement for conventional linear elastic materials, the dynamic modulus can exhibit substantially higher modulus values than quasistatic measurements for materials showing nonlinear hysteretic behavior. The objective of this paper is to show that these measurements can be reconciled and a consistent picture of the elastic response of plasma-sprayed coatings can be established.

This is a preprint or reprint of a paper intended for presentation at a conference. Because changes may be made before formal publication, this is made available with the understanding that it will not be cited or reproduced without the permission of the author.

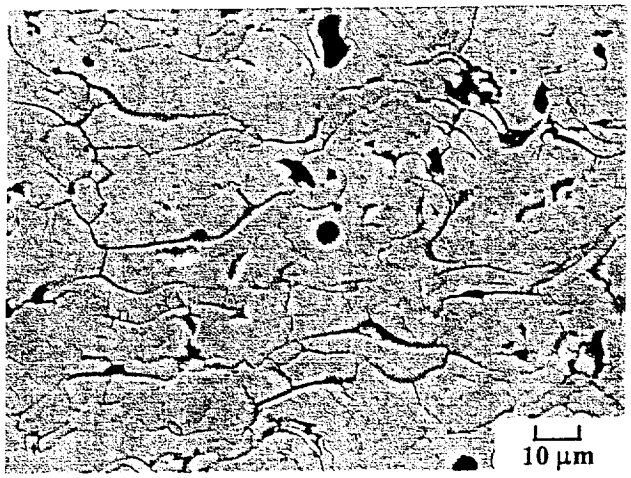

Figure 1. SEM micrograph of polished cross section of plasma-sprayed 8YSZ TBC. Plasma-spray direction is from top to bottom.

EXPERIMENTAL PROCEDURE

Flat-bottomed cylindrical punch (127 μm diameter) instrumented indentations were performed at room temperature on cross sections of 1.5 mm thick plasma-sprayed ZrO_2-8wt%Y_2O_3 (8YSZ) coatings that had been sprayed onto a 0.25 mm thick Fe-25wt%Cr-5wt%Al-5wt%Y bond coat which in turn had been sprayed onto a 4140 steel substrate. Details of the testing procedure, apparatus, and modulus determination have been reported.[5] The primary advantage of the flat-bottomed cylindrical punch (as compared to pointed indenters) is that the indentation contact area remains constant throughout the test so that the applied stress is simply proportional to the applied load. Elastic modulus values are determined from the compliance-corrected data using the relationship $E = (dP/dh) \times (1-\nu^2)/2r$ where E is the coating elastic modulus, P is the applied load, h is the compliance-corrected indenter displacement, ν is the coating Poisson ratio, and r is the indenter radius.

Uniaxial compression and sound velocity measurements were performed on 3.4 mm x 4.0 mm x 50 mm rectangular beams that had been machined from plates of plasma-sprayed 8YSZ after etching away the 4140 steel substrate. Uniaxial compression tests were conducted at room temperature; a strain gage with a gage length of 18 mm was attached to the specimen. Instantaneous (tangential) modulus values were determined from the slope of the stress-strain curve. Sound velocity measurements were performed using a pair of acoustic emission (AE) transducers mounted 15 mm apart along the 50-mm axis on the same face of the specimen. These measurements were performed while the specimen, mounted in a load frame, was under controlled compression along its long axis. Sound velocities were determined by dividing the inter-transducer distance by the time interval between the sound wave arrival at the two AE transducers; sound waves were generated by breaking a boron fiber against the specimen outside the length spanned by the two transducers. The elastic modulus was determined from the relationship $E = \rho(1-\nu^2)C_e^2$, where E is the elastic modulus, ρ is the coating density (5.1 g/cm^3), ν is the Poisson ratio (0.2), and C_e is the extensional sound velocity.

RESULTS

After preloading to 35 N (2.76 GPa) to inhibit time-dependent deformation during testing, cylindrical punch indentations were performed on the polished cross section of a plasma-sprayed 8YSZ TBC. Each test consisted of three load/unload cycles up to a maximum load of 30 N (2.37 GPa applied stress) with a 10 sec hold at maximum load. A plot of a typical indentation test (Fig. 2a) clearly displays very repeatable (except for a small deviation for the first loading) nonlinear elastic behavior with hysteresis. Instantaneous elastic modulus values were calculated (Fig. 2b) from the loading/unloading slopes over a load range from 5 N (0.39 GPa applied stress) to 30N (2.37 GPa applied stress). Data points with loads under 5 N were not used due to indenter seating effects. The plot shows that during loading the instantaneous modulus increases modestly from 50 to 65 GPa, experiences a significant upward jump upon loading/unloading reversal up to modulus value of 83 GPa, and then decreases more rapidly during unloading than it increases during loading down to a modulus value of 42 GPa. It should be noted that the instantaneous modulus determined during initial unloading is higher than at any other point in the cycle.

Uniaxial cyclic compression tests were performed up to a maximum load of 900 N (46 MPa applied stress) on the rectangular beam plasma-sprayed 8YSZ specimens. A plot of a typical compression cycle (Fig. 3a) shows nonlinear hysteretic elastic behavior similar to that observed during indentation (Fig. 2a), albeit at significantly higher applied stresses. Instantaneous elastic modulus values were calculated (Fig. 3b) from the loading/unloading slopes over a range from 10 to 46 MPa applied stress. Data points with applied stress under 10 MPa were not used due to fixture seating effects. The plot shows that during loading the instantaneous modulus increases from 14 to 32 GPa and then jumps up to 49 GPa, followed by a rapid decrease during unloading down to a modulus of 12 GPa.

Dynamic elastic modulus values determined by sound velocity measurements also showed very nonlinear elastic behavior for the rectangular beam plasma-sprayed 8YSZ specimen (Fig. 4). Modulus values were observed to increase significantly from a value of 25 GPa with no applied stress up to 68 GPa at an applied compressive stress of 74 MPa. The rate of modulus increase was observed to decrease with increasing compressive stress. In contrast, modulus values determined by sound velocity measurements for dense SiC, Si_3N_4, and Al_2O_3 specimens showed no significant dependence on applied compressive stress, typical of linear elastic behavior. Unlike the indentation and uniaxial compression results, however, no significant hysteresis was observed between sound velocity measurements acquired during loading vs. unloading sequences. In addition, where the applied compressive stress ranges overlapped between the sound velocity and uniaxial compression tests, the modulus values determined from sound velocity measurements were generally higher (Figs. 3b, 4).

An effort was made to see if dynamic-like measurements could be obtained from indentation and uniaxial compression tests by incorporating short internal load reversal loops into the larger overall load/unload cycle. Because the indentation tests differed from the uniaxial compression and sound velocity tests in being performed at compressive stresses that were much higher and applied parallel instead of perpendicular to the plasma-spray direction, only the results from the uniaxial compression testing will be shown here, providing a direct comparison with the sound velocity measurements. Fig. 5 shows a plot of such a test, where the overall compression cycle was performed to a maximum of 46 MPa applied stress as before (Fig. 3a), but now includes eight 100-N amplitude internal load reversal loops that are performed symmetrically between the loading and unloading halves of the cycle. Inspection of the load reversal loops (Fig. 5) reveals that the average slope of these loops increases with increased applied stress, and that the pairs of load reversal loops spanning the same load range (one during loading, the other during unloading) have parallel slopes, indicating an absence of hysteresis. An absence of hysteresis is confirmed

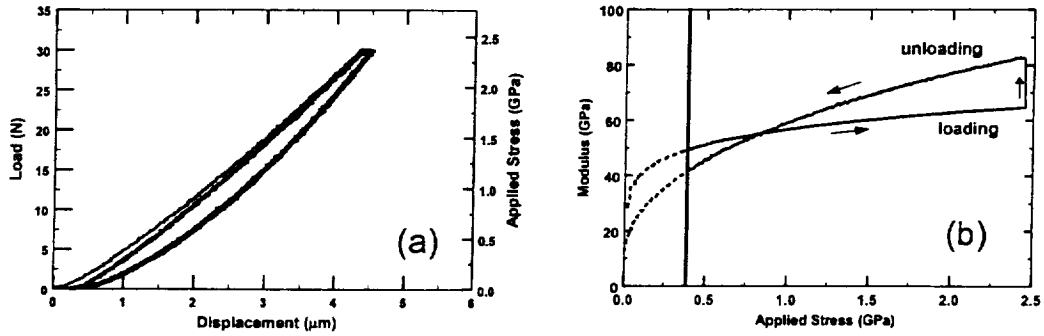

Figure 2. (a) Typical set of three consecutive cylindrical punch loading/unloading cycles performed on polished section of plasma-sprayed 8YSZ TBC. (b) Calculated instantaneous modulus vs. applied compressive stress determined from final indentation cycle.

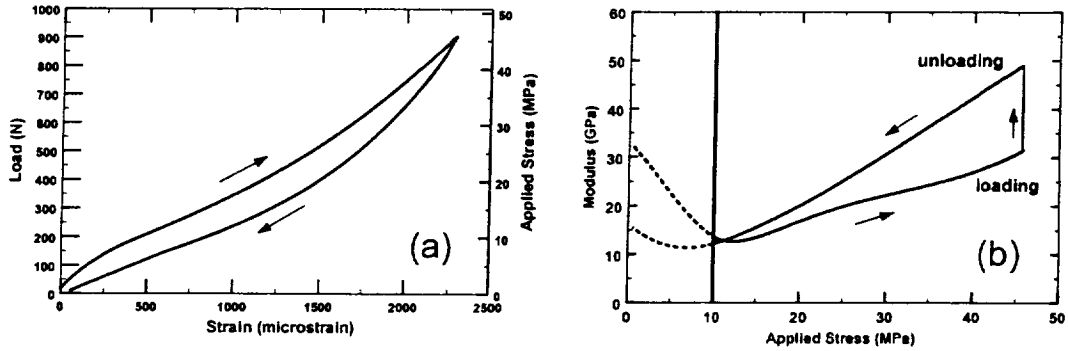

Figure 3. (a) Typical stress-strain curve in uniaxial compression for rectangular beam of plasma-sprayed 8YSZ. (b) Calculated instantaneous modulus vs. applied compressive stress.

from the modulus values determined from the average slopes of the load reversal loops, which are plotted in Fig. 6 along with modulus values determined from the sound velocity measurements and from the uniaxial compression tests without internal load reversal loops.

DISCUSSION

While the TBC specimens are elastic in the sense that they exhibit complete strain recovery as evidenced by closed loop cyclic loading behavior (Figs. 2a, 3a), this elasticity is not associated with atomic scale bonding. Because the elastic response of the plasma-sprayed 8YSZ TBCs are instead largely governed by contact between subelements of its microcracked lamellar microstructure (Fig. 1), the elastic response cannot be described by a single-valued Young's modulus. As previously proposed,[2,5] the coating stiffens under increasing applied compressive stress due to the increasing contact area between subelements. Once static friction is overcome, contacting internal surfaces also experience frictional sliding, which reduces coating stiffness, and causes hysteresis because static friction must be overcome again before reverse internal sliding

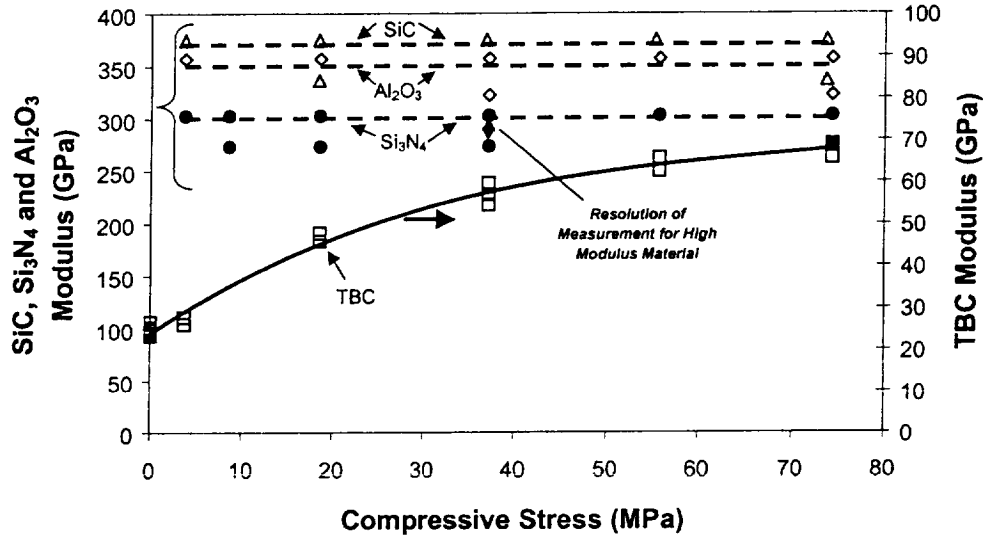

Figure 4. Modulus determined from sound velocity measurements as a function of applied compressive stress for rectangular beam of plasma-sprayed 8YSZ as well as dense beams of SiC, Si_3N_4, and Al_2O_3.

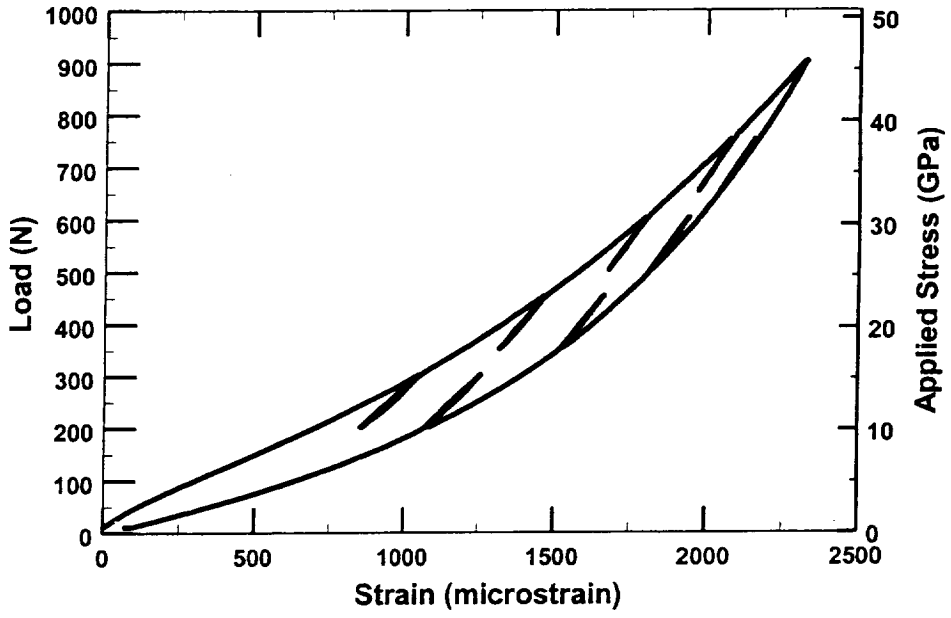

Figure 5. Uniaxial compression stress-strain curve incorporating 100-N amplitude load reversal loops.

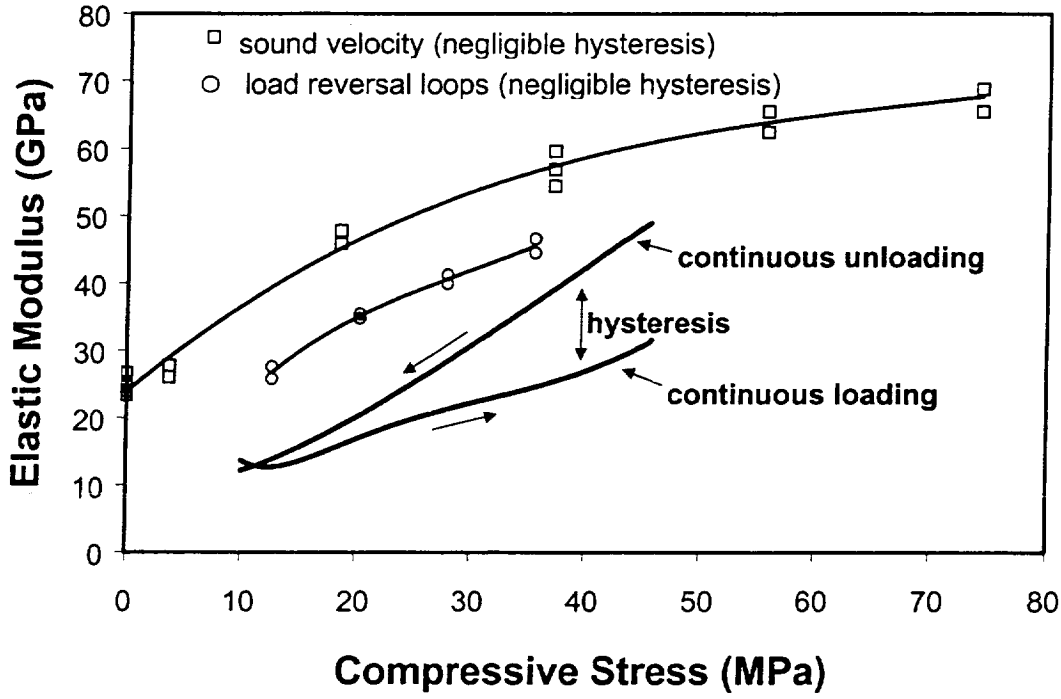

Figure 6. Comparison of elastic modulus measurements of plasma-sprayed 8YSZ obtained by sound velocity measurements, standard uniaxial compression measurements, and from short load reversal loops incorporated into uniaxial compression measurements.

can proceed. Rejda, Socie, and Itoh[2] have proposed a mechanistic model based on local crack closing and internal sliding surface mechanisms to provide a qualitative model of the elastic response of plasma-sprayed TBCs. Another approach for quantitatively predicting the elastic response of plasma-sprayed TBCs is a more generalized analysis that models the TBC by a distribution of gaps where the gap closing stress is greater or equal to the gap opening stress;[6,7] the difference in closing and opening stress simulates the requirement of overcoming static friction when the direction of internal sliding is reversed. Once the distribution of opening and closing stresses is determined, the elastic response to any sequence of applied stresses can be predicted.

In view of the current understanding of the microstructure-governed elastic behavior of plasma-sprayed TBCs, the apparently inconsistent quasistatic and dynamic modulus measurements (Fig. 6) presented here can be reconciled. Each modulus measurement is then best understood as the microstructural response to the specific applied stress protocol associated with that test. For the quasistatic indentation and uniaxial compression tests (Figs. 2 and 3), the high strain amplitude, monotonic loading and unloading segments include significant contributions from internal sliding that reduce the measured instantaneous modulus below what would be observed without internal sliding; internal sliding also produces the pronounced hysteresis associated with the quasistatic modulus measurements in Fig. 6. In contrast, for the dynamic sound velocity modulus measurements (Fig. 6), the high-frequency stress fluctuations associated with sound wave propagation do not produce sufficiently high strain changes to overcome static friction during the stress fluctuations. Therefore, the modulus-reducing and hysteresis-producing effects of internal

sliding are absent, consistent with the higher modulus values and lack of hysteresis observed in the sound velocity measurements. (Fig. 6)

Finally, the hysteretic effects of internal sliding could be substantially reduced in the quasistatic measurements by incorporating short load reversals into the larger loading cycle. (Figs. 5, 6) For short load reversals, internal sliding is greatly reduced because of the requirement of overcoming static friction. As observed in Fig. 6, the modulus values determined from the load reversal loops mimic the sound velocity measurements in showing the same curvature and lack of hysteresis, although at somewhat lower modulus values.

CONCLUSIONS

Plasma-sprayed TBCs exhibit nonlinear hysteretic elastic behavior that cannot be described by a single-valued Young's modulus. This nonlinear elastic behavior is governed by the internal contact surfaces within the coating's plasma-spray microstructure and produces apparent discrepancies between quasistatic (indentation and uniaxial compression) and dynamic (sound velocity) modulus measurements. These apparent discrepancies can be reconciled by realizing the significant effects of internal surface sliding in the quasistatic modulus measurements compared to the relative absence of effects of internal sliding in the dynamic modulus measurements. The consistency of the measurements was confirmed by making the quasistatic uniaxial compression tests "dynamic-like" by incorporating short load reversals during which internal surface sliding was inhibited.

ACKNOWLEDGMENTS

The authors wish to thank R.A. Miller and D. Zhu for helpful discussions and Q. Nguyen for assistance with SEM.

REFERENCES

1. J.T. DeMasi-Marcin, K.D. Sheffler, and S. Bose, "Mechanisms of Degradation and Failure in a Plasma-Deposited Thermal Barrier Coating," ASME J. Eng. Gas Turbines Power, **112**, 521-26 (1990).
2. E.F. Redja, D.F. Socie, and T. Itoh, "Deformation Behavior of Plasma-Sprayed Thick Thermal Barrier Coatings," Surf. Coatings Technol., **113**, 218-26 (1999).
3. S.R. Choi, D. Zhu, and R.A. Miller, "High-Temperature Slow Crack Growth, Fracture Toughness, and Room-Temperature Deformation Behavior of Plasma-Sprayed ZrO_2-8wt% Y_2O_3," Ceram. Eng. Sci. Proc., **19**[4] 293-301 (1998).
4. S.R. Choi, D. Zhu, and R.A. Miller, "Deformation and Strength Behavior of Plasma-Sprayed ZrO_2 8wt% Y_2O_3 Thermal Barrier Coatings in Biaxial Flexure and Trans-Thickness Tension," Ceram. Eng. Sci. Proc., **21**[4] 653-61 (2000).
5. J.I. Eldridge, D. Zhu, and R.A. Miller, "Mesoscopic Nonlinear Elastic Modulus of Thermal Barrier Coatings Determined by Cylindrical Punch Indentation," J. Amer. Ceram. Soc., **84**[11] 2737-39 (2001).
6. R.A. Guyer and P.A. Johnson, "Nonlinear Mesoscopic Elasticity: Evidence for a New Class of Materials," Physics Today, **52**[4] 30-36 (1999).
7. K.R. McCall and R.A. Guyer, "Equation of State and Wave Propagation in Hysteretic Nonlinear Elastic Materials," J. Geophys. Res., **99**[B12] 23887-23897 (1994).